

**Alex Pokryvailo and Costel Carp**

*Spellman High Voltage Electronics Corporation  
475 Wireless Boulevard  
Hauppauge, NY 11788*

## ***Comparison of the Dielectric Strength of Transformer Oil Under DC and Repetitive Multimillisecond Pulses***

Copyright © 2012 IEEE. Reprinted from IEEE Electrical Insulation Magazine, May/June 2012— Vol. 28, No. 3

This material is posted here with permission of the IEEE. Such permission of the IEEE does not in any way imply IEEE endorsement of any of Spellman High Voltage Electronics Corporation's products or services. Internal or personal use of this material is permitted. However, permission to reprint/republish this material for advertising or promotional purposes or for creating new collective works for resale or redistribution must be obtained from the IEEE by writing to [pubs-permissions@ieee.org](mailto:pubs-permissions@ieee.org).

By choosing to view this document, you agree to all provisions of the copyright laws protecting it.

# *Comparison of the Dielectric Strength of Transformer Oil Under DC and Repetitive Multimillisecond Pulses*

**Key words:** transformer oil, millisecond pulses, high voltage, power supply

## **Introduction**

The dielectric strength of insulating liquids in general, and of transformer oil in particular, is of great practical interest and has been studied extensively for more than a century [1]–[6]. Reference [7] focuses on the impulse breakdown of liquids over a wide range of parameters and is particularly relevant to the work presented in this article.

It is well known that the dielectric strength of fresh, thoroughly purified (filtered, degassed, dehumidified) oil is several times higher than that of aged, contaminated oil, except under nano- or picosecond pulses. Some of the reasons for this difference are as follows: (1) under the influence of an electric field, solid impurity particles or water may form a chain and initiate breakdown [1]; (2) solid impurities can be generated in oil as the result of accidental or intentional arcs, or oxidation of metals; (3) water may be absorbed from the atmosphere in non-hermetically sealed devices.

The various breakdown mechanisms have been discussed extensively [1]–[7]. In highly purified liquids, breakdown is usually governed by micro-defects, e.g., gas cavities of nano- and micrometer size trapped on electrode surfaces and in bulk liquid. Even in the absence of micro-bubbles, a transition from liquid to gas can occur owing to heating by electrons field-emitted from the cathode. Because the dielectric strength of a gas is much lower than that of the corresponding liquid, discharge is initiated in the gas and can progress to full breakdown through the bulk liquid. For details, see Ch. 2 of [7]. In contaminated, aged liquids, breakdown mechanisms are less subtle, e.g., a mechanism in which foreign particles tend to align along the electric field lines, building a bridge that initiates discharge. However, this mechanism operates typically on millisecond time scales because of the slow associated particle movement [4]–[7].

Oil degrades considerably in equipment that has been in service for extended periods. In equipment with sealed tanks, e.g., x-ray monoblocks [8], the oil would probably not be changed during the lifetime of the equipment. In such circumstances, breakdown mechanisms and the dielectric strength of purified

## **A. Pokryvailo and C. Carp**

*Spellman High Voltage Electronics Corporation, 475 Wireless Boulevard Hauppauge, NY 117*

*The dielectric strength of fresh and contaminated transformer oil under repetitive millisecond pulses was compared with that at DC voltage. The pulsed breakdown voltage was found to be higher than its DC counterpart by 10 to 20%.*

fresh oil are irrelevant, except possibly for the initial choice of oil. Working field stress is chosen on the basis of expected breakdown stress at the end of the service lifetime. A vast database exists on the dielectric strength of fresh and aged oils under DC, AC, and pulsed stress, e.g., [1]–[7] and their references.

As with any dielectric, the breakdown voltage (BV) of liquids tends to increase under short pulses, although not consistently [5], [9]. It was reported in an early investigation [9] that, for transformer oil, the BVs under pulses of several milliseconds duration and very low pulse repetition rates (PRRs) were higher than for AC (60 Hz) by a factor of approximately 1.5 to 2, with larger increases for shorter pulses.

In some equipment, oil is subjected to repetitive pulse stress. Despite the huge amount of breakdown voltage data, we could not find an explicit comparison of the dielectric strength of oil at AC or DC voltages with that under repetitive millisecond pulses.

Table 1. High-Voltage Power Supply Basic Specifications.	
Input voltage	90 to 264 VAC, 50/60 Hz (or 0 to 420 VDC if bypassing input rectifier and power factor corrector)
Output voltage	0 to 160 kV (0 to $\pm 80$ kV bipolar symmetric to ground)
Output current	0 to 12 mA
Pulse repetition rate	DC, or single shot up to 150 Hz (limited by fall time)
Rise time to nominal voltage	<1 ms without shielded HV cables
Output capacitance	About 30 pF (not including shielded HV cables)
Fall time	Load and HV cable dependent
Ripple, peak to peak	<2%
Conversion frequency	150 kHz
Size	15.7 $\times$ 34.3 $\times$ 45.7 cm
Insulation	Transformer oil

Because the insulation thickness in equipment used for many specialized applications, e.g., x-ray machines, is much less than that commonly found in power equipment, e.g., transformers and switchgear, information on dielectric strength under repetitive millisecond pulses is important. These two factors motivated the investigation reported below.

## Setup and Methods

### A. High-Voltage Power Supply

The basic parameters of the custom-designed switch-mode high-voltage power supply (HVPS) are summarized in Table 1. It generates bipolar voltage pulses symmetrical to ground (zero to  $\pm 80$  kV) at PRRs up to 150 Hz. Arc fault detection and consequent shutdown are provided. Although the HVPS can be fed directly from mains, we preferred feeding its DC-to-DC converter from a regulated DC power supply (one of a Spellman SL series [10]). This enabled greater HV control flexibility. The output was delivered through two shielded cables, each approximately 3 m in length, or by two unshielded cables, each approximately 2 m in length. The importance of specifying the output exactly is that the HV cable capacitance affects the pulse fall time greatly, thus limiting the PRR.

The HVPS with unshielded polyethylene cables attached is shown in Figure 1, along with two function generators setting the PRR and ramp rate (see Test Procedures below). It is a standard Spellman package comprising low-voltage (LV) and high-voltage (HV) sections. The LV section contains a line rectifier, power factor corrector, inverter, and control board. The HV unit houses the HV transformers, multipliers, feedback dividers, et cetera, and is oil-insulated.

A typical negative pole output relative to ground at full voltage (75 kV, or 150 kV between the poles), as measured by the feedback divider, is shown in Figure 2. The flatness of the bottom of the pulse, as observed in calibration tests against a Tektronix P6015A HV probe (Tektronix Inc., Beaverton, OR) up to 40 kV, is better than that shown in Figure 2. The limiting

factor in raising the PRR is the discharge time of the cables. (The multiplier capacitance of approximately 30 pF can be neglected.)

### B. Device Under Test

We chose a sphere-to-plane spark gap (SG) configuration to imitate the operational conditions of x-ray tubes and other HV parts in oil. The field nonuniformity factor  $f$ , defined as

$$f = E_m/E_{av}, \quad (1)$$

where  $E_m$  and  $E_{av}$  are respectively the maximum and the average field in the gap, would be typically in the range of 1.5 to 6 in the imitated systems. The lower values relate to large, low-curvature

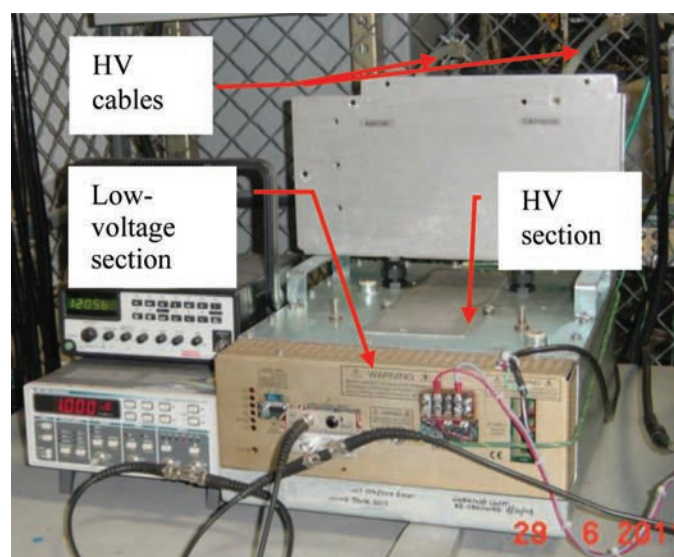


Figure 1. High-voltage power supply (HVPS) with unshielded polyethylene cables.

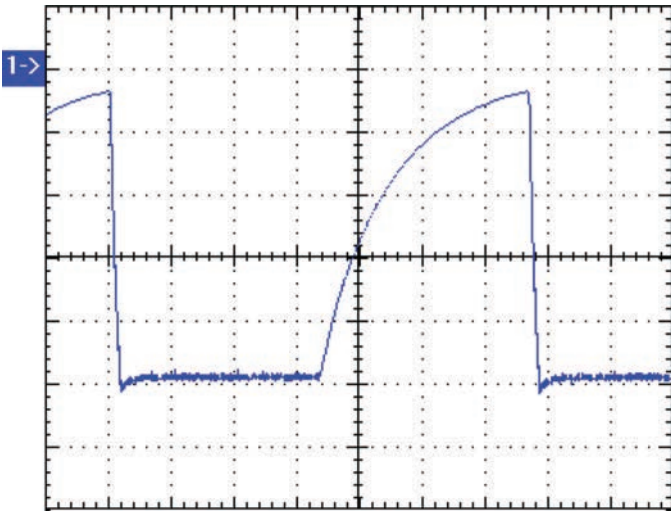


Figure 2. Typical output of the negative pole ( $-75\text{ kV}$ ), with shielded cables. Load resistance =  $83.5\text{ M}\Omega$ . Pulse repetition rate =  $15\text{ Hz}$ . Vertical scale  $15\text{ kV/div}$ , with zero indicated by  $1\rightarrow$ ; horizontal scale  $10\text{ ms/div}$ .

electrodes, and the larger values relate to ball-soldered joints of components such as diodes, resistors, and capacitors.

The test SG is shown in Figure 3. The polished brass sphere has a  $12.5\text{ mm}$  diameter, and the plane is formed by a  $20\text{-mm}$ -thick,  $63.4\text{-mm}$ -diameter aluminum disc rounded on the edges. Sturdy Lexan stands, reinforced for rigidity, support the electrodes; the gap can be varied between  $0$  and  $40\text{ mm}$  using a threaded rod. Practical test gaps, however, were limited to  $15\text{ mm}$  by the voltage capabilities of the HVPS. Field analysis (see Appendix) showed that the field nonuniformity factor  $f$  in the practical test gaps varied from unity to slightly greater than  $3$ . We note here that the electric field inside a sphere-to-plane gap for a symmetrical connection (bipolar voltage application) is very similar to that for a grounded plane.

For testing, we chose a Shell Diala A/AX oil (Shell Oil Company, Houston, TX) widely used in industry. The dielectric



Figure 3. Sphere-to-plane spark gap.

Year	Average BV (kV)	Standard deviation (kV)	Oil condition
2010	34.0	6.1	Fresh
2010	14.8	2.3	Contaminated
2011	40.3	4.0	Fresh

strength at  $60\text{ Hz}$  was determined in accordance with ASTM D 1816-84a [11] for fresh oil (before the tests) and for contaminated oil (after the tests). The results are presented in Table 2. Two oil batches, each of approximately  $20\text{ L}$ , were used for the three tests listed in the table. One batch was used in 2010 and another in 2011.

### C. HV Layout

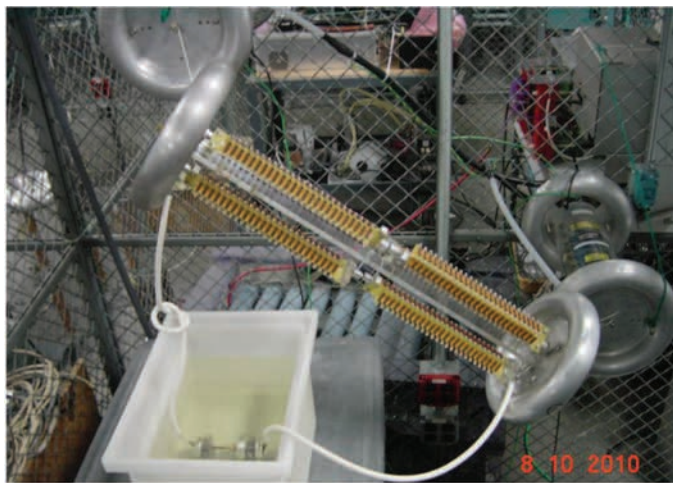
The SG was immersed in about  $20\text{ L}$  of oil contained in a plastic tank (Figure 4). A bleeder load was connected to the HVPS to assist the discharge, and bare silicone rubber HV leads connected the HVPS donuts to the SG. At first, no limiting resistors were used, but after tests with fresh oil (see Fresh Oil section), an assembly consisting of five  $22\text{-k}\Omega$  resistors connected in series was mounted on each pole to limit the discharge current. These assemblies were used only with shielded HV cables. In the case of unshielded HV cables, no limiting resistors were needed in view of the small amount of stored energy. With shielded cables, the load was  $83.5\text{ M}\Omega$ . With unshielded cables, pulsed tests were conducted using a  $20\text{-M}\Omega$  load, which allowed testing at PRRs up to  $120\text{ Hz}$ .

The polarity was switched by swapping the leads. Thus, all the tests were conducted under a bipolar voltage application (symmetrical connection).

### D. Test Procedures

All tests were conducted at room temperature. The voltage was increased linearly at a rate of  $4\text{ kV/s}$  until breakdown occurred, or up to a maximum of  $150\text{ kV}$ , either by programming the Spellman SL power supply (for measurements with shielded cables), or by programming the HVPS (for measurements with unshielded cables). In the first case, the HVPS operated with an open feedback loop, and in the second case with a closed feedback loop, which yielded tighter regulation of the output voltage amplitude and a flatter pulse top. If breakdown did not occur before the maximum voltage was reached, the voltage was then linearly reduced at  $4\text{ kV/s}$ . The tests for each gap spacing were performed for each of the following voltage waveforms:

- 1) positive polarity, marked as DC+ (sphere positive);
- 2) negative polarity, marked as DC- (sphere negative);
- 3) positive polarity pulsed, marked as Pulsed+ (sphere positive);
- 4) negative polarity pulsed, marked as Pulsed- (sphere negative).



(a)



(b)

Figure 4. HV layout. (a) Shielded HV cables (partially visible). The load is supported by two HV dividers, HVD100 [12], allowing measurement of the voltage between the poles and ground. (b) Unshielded polyethylene cables. A resistive load shortens the voltage impulse fall time.

For waveforms 3 and 4, the ramp voltage modulated the pulsed output. At a PRR of 10 Hz the duty cycle  $D$  was 50%, and 20% at PRRs of 30, 50, and 120 Hz.

An interval of at least 1 min was maintained between successive tests, in line with oil testing procedures [11], [13]. Seven breakdown tests were performed for each of the four test types, and the average and standard deviation values were calculated. If the voltage application did not result in breakdown, a BV of 150 kV was assigned to the relevant test. The electrodes were cleaned after each change of gap distance.

The BV in DC tests was determined by a Fluke 179 multimeter (Fluke Corporation, Everett, WA) using its MaxMin function (capturing the maximum value). In pulsed tests, the BV values were recorded by a TDS3034C oscilloscope (Tektronix Inc.). Its horizontal sweep was set in such a way as to capture a few of the last pulses before breakdown. The BV value was taken as the

peak of the feedback divider signal if the breakdown took place on the rising edge or at the crest, or as the amplitude of the “flat” top (disregarding overshoot, if any) if the breakdown occurred at the top or on the trailing edge. The crest value of the envelope of the same signal, on a 10 s/div time base scale, was also recorded. In open-loop operation, the pulse top drooped considerably because of the limited power of the DC power supply; in closed-loop operation, the pulse top was essentially flat.

## Test Results

### Fresh Oil (Shielded Cables)

The first test series was conducted with fresh oil without limiting resistors at the output of the cables. At a PRR of 10 Hz, breakdowns occurred mainly on the flat top or during the pulse tail. The results are summarized in Figure 5. As expected, BV at negative polarity was higher than at positive polarity. This was the case for gas, liquid, and solid insulation, and for many electrode shapes, gap sizes, and voltage waveforms. A succinct summary of the polarity effect can be found in [5]. There was no clear difference between pulsed and DC breakdown. The BV standard deviation was considerably larger for positive polarity than for negative polarity.

### Contaminated Oil (Shielded Cables)

#### (1) Contamination Attributable to Arcing

After tests with fresh oil, the limiting resistors described in Section IIC were installed on the electrodes as shown in Figure 6 (five 22-k $\Omega$  resistors on each pole). At the smallest gap, the arc fault trip did not operate following the first breakdown, so

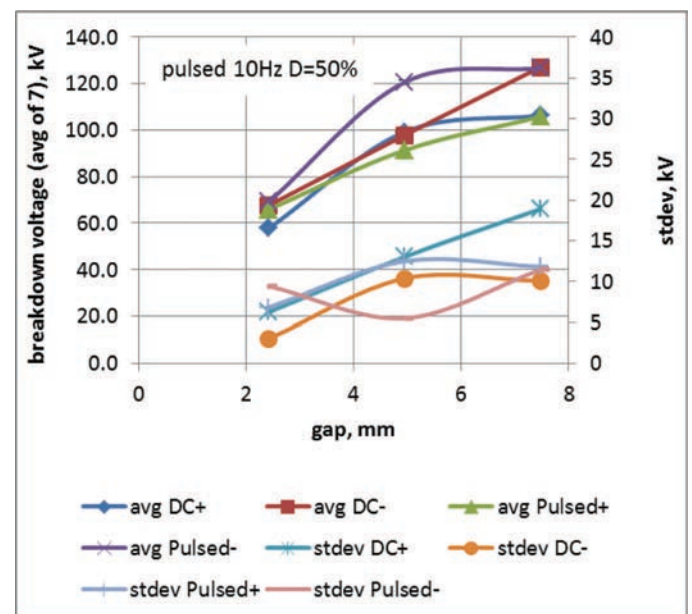


Figure 5. Breakdown voltages for fresh oil, without limiting resistors at the output of the cables. Pulse repetition rate (PRR) = 10Hz,  $D$  = duty cycle = 50%.

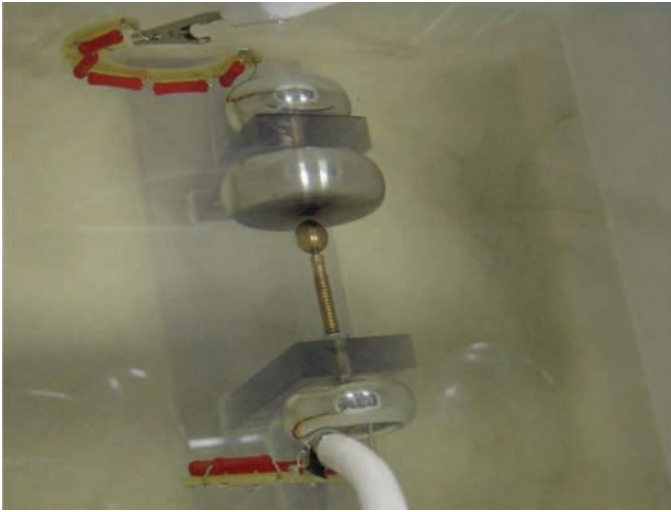


Figure 6. Limiting resistors (in red) attached to the electrodes. Note the soot floating in the oil.

the unit arced many times, sometimes for 1 to 2 s, before shutting down. Because all the charge stored in the cable capacitance passed through the arc channel during every discharge, the oil was blackened with soot despite a low peak current (Figure 6), and its BV, as tested by the standard method, decreased markedly (Table 2).

Two series of tests were performed with the soot-contaminated oil. In the first, the voltage parameters were the same as before, i.e., PRR = 10 Hz and D = 50%. In the second series, PRR = 30 Hz and D = 20% were selected to investigate the influence of the pulse width. A typical set of waveforms at breakdown for the second series is shown in Figure 7. The oscilloscope was triggered on the falling (trailing) edge of the last pulse (pulse on which the breakdown occurred); all breakdowns occurred either

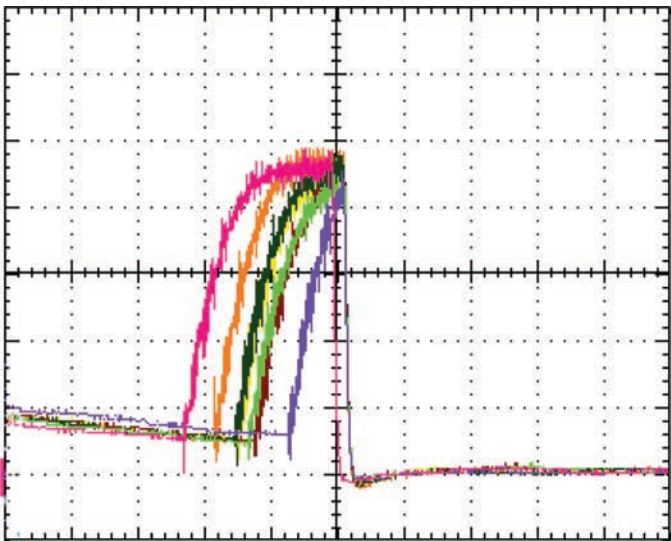


Figure 7. Last pulse at breakdown for a 10-mm gap, negative polarity, oil contaminated by arcing. PRR = 30 Hz, D = 20%. Horizontal scale 2 ms/div, vertical scale 30 kV/div.

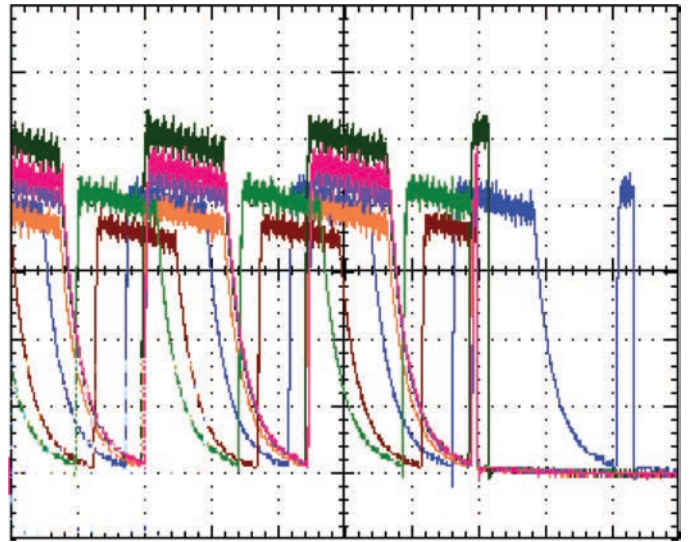


Figure 8. Last pulses before breakdown for a 7.47-mm gap, negative polarity, oil contaminated by arcing. PRR = 10 Hz, D = 50%. Horizontal scale 40 ms/div, vertical scale 30 kV/div.

on the rising (leading) edge or immediately after the crest, but for longer pulses of the first series, they occurred mainly on the “flat” top (Figure 8).

The results are presented graphically in Figures 9 and 10. Again, the BV was higher at negative polarity than at positive polarity (the 15.2-mm gap did not arc in most of the tests up to 160 kV), and the standard deviation was smaller. However, there was a marked difference between pulsed and DC breakdown at both polarities; the average pulsed BV was higher than its DC counterpart by 14.9% for positive polarity, and by 10.3% for negative polarity. We attribute this difference to the bridge breakdown mechanism in contaminated liquids [1]–[2], [4]–[7]. The contaminating particles take some time to form a bridge along the field direction, and initiate breakdown. However, there is no clear difference between long and short pulses (Figure 10).

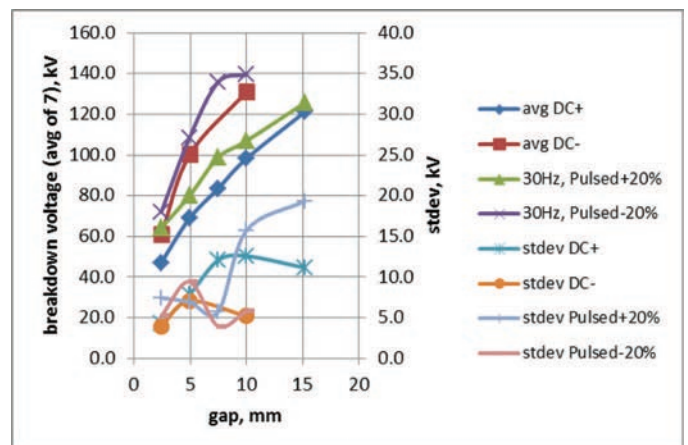


Figure 9. The BV for oil contaminated by arcing. PRR = 30 Hz, D = 20%.

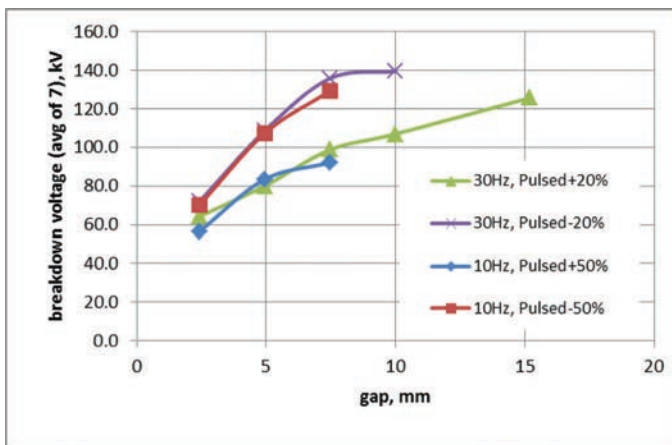


Figure 10. The BV for oil contaminated by arcing. PRR = 30 Hz with  $D = 20\%$ , and PRR = 10 Hz with  $D = 50\%$ .

## (2) Contamination with Soot and Other Additives

An even greater decrease in dielectric strength might be expected for heavily contaminated (aged) oil, compared with fresh oil and soot-contaminated oil. Because contamination of the oil through conventional commercial usage would be too slow, we opted to add other contaminants with well-defined properties. Two sets of samples were prepared as follows:

- 4 mL (approximately 0.24 g) of fine silica (Degussa R812, hydrophobic, particle size 8 nm, also known as Aerosil R 812, Evonik Degussa GmbH, Essen, Germany) was thoroughly mixed with 20 L of the soot-contaminated oil used in the measurements described above.
- In addition to the fine silica particles, 4 mL of a silicone-based paste containing nano-sized carbon black (Dispersion Technology Inc., Bedford Hills, NY; color K-73169, average particle size 42 nm) was then added and stirred until uniformly dissolved, blackening the oil and rendering it almost opaque.

BV measurements were made only on a 15.2-mm SG at positive polarity because no dramatic change in dielectric strength, compared with that measured on samples contaminated only with soot, was found.

Although silica reduced the BV to some extent, carbon black increased it (Table 3). Possible explanations for the increase are as follows:

- Oil containing conductive or semiconductive nanofillers has greater breakdown strength than oil without nanofillers [14]–[16].
- Field nonuniformity decreases with increasing conductivity.

## Contaminated Oil (Unshielded Cables, 2011)

Measurements were made on a new batch of oil that had been contaminated by soot formed during prolonged arcing in preliminary tests. The aim was to investigate whether PRRs above 30 Hz had a greater effect on dielectric strength than those that had been observed up to 30 Hz. Accordingly, the time intervals between successive tests were kept as short as possible; i.e., a positive DC test was followed immediately by a pulsed DC test, or vice versa. The gap width and the arrangement of the leads were not modified, so that the oil was not stirred and its condition remained very largely unchanged between tests. Thus a meaningful comparison between DC and pulsed tests was possible; a comparison of results obtained days apart would be questionable.

Unshielded HV cables, heavier loads, and closed-loop operation allowed testing at higher PRRs with cleaner waveshapes. Figure 11(a) shows, for PRR = 50 Hz, a typical last pulse prior to breakdown, and the following pulse on whose flat top the breakdown took place. Traces 1 and 3 in Figure 11(b) show pulses during which breakdown occurred, at PRR = 120 Hz. The rise times of these pulses are less than 1 ms, whereas trace 2 shows that the trailing edge of a pulse during which breakdown did not occur was approximately 7 ms in duration. Breakdowns were observed only along the leading edge or the flat top, never along the trailing edge.

The test results are summarized in Figure 12. Figure 12(c) is constructed using the breakdown voltages shown in Figures 12(a) and 12(b), omitting standard deviations in the interests of clarity. In Figure 12(c), (50) or (120) indicate that the breakdown voltages at DC were measured in successive tests with their pulsed counterparts at 50 or 120 Hz, respectively. Thus avg DC+(120) means that positive DC breakdown voltages were measured immediately before or after pulsed tests at positive polarity and at 120 Hz (avg Pulsed+120Hz) for each gap width. Thus the oil was not stirred between these tests (as it would be if the gap were changed or the leads swapped).

Clearly, the BVs for the pulsed waveform at both 50 and 120 Hz are considerably higher than their DC counterparts. Figure 12(c) shows that the breakdown field,  $E_{br}$ , decreases sharply with increasing field nonuniformity factor  $f$ . The latter is calculated for the geometry shown in Figure 14 of the Appendix.

Test type	Average BV (kV) for oil contaminated with soot and other additives	Average BV (kV) for oil contaminated only with soot
DC+	116 (soot + silica)	121
DC+	127 (soot + silica + carbon black)	121
Pulsed+, 30 Hz, $D = 20\%$	132 (soot + silica)	125.7
Pulsed+, 30 Hz, $D = 20\%$	130 (soot + silica + carbon black)	125.7

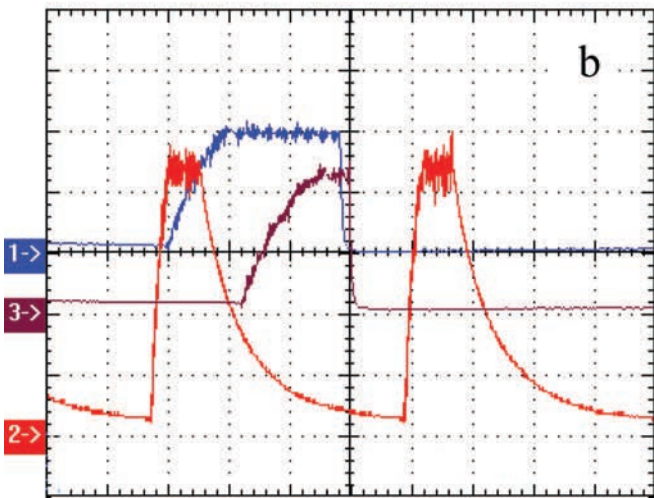
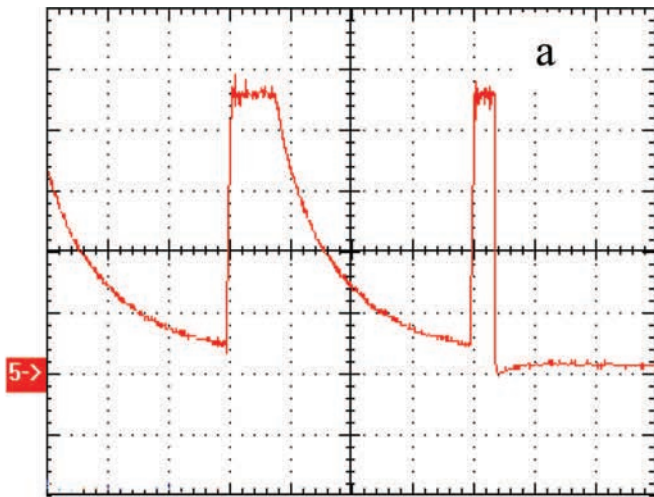
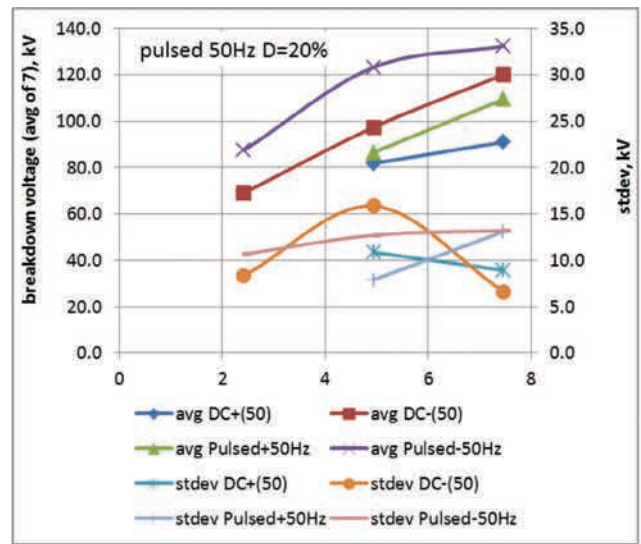


Figure 11. Typical pulse waveforms. (a) The last pulse prior to breakdown, followed by the pulse during which breakdown occurred. Gap = 7.47 mm, load = 82 M $\Omega$ , negative polarity, PRR = 50 Hz, horizontal scale = 5 ms/div, vertical scale = 30 kV/div. 5→ indicates the zero on the vertical axis. (b) Traces 1 and 3 show pulses on which breakdown occurred, with horizontal scale 0.5 ms/div, vertical scale 60 kV/div. Trace 2 shows the long trailing edge of a pulse when breakdown did not occur, horizontal scale 2 ms/div, vertical scale 30 kV/div. 1→, 2→, and 3→ show the zeros on the vertical axis for the corresponding traces. Gap = 4.94 mm, load = 20 M $\Omega$ , negative polarity, PRR=120 Hz.

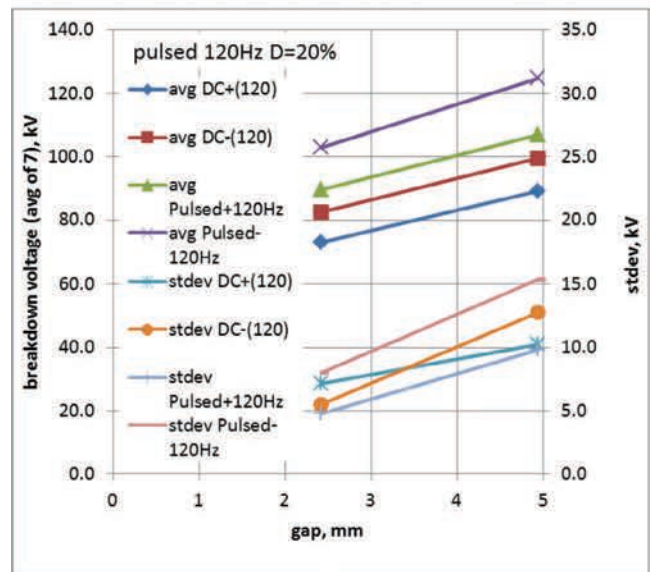
Table 4, in which the results of all the tests are drawn together, shows that the breakdown voltage is consistently higher under pulsed conditions than at DC.

## Conclusion

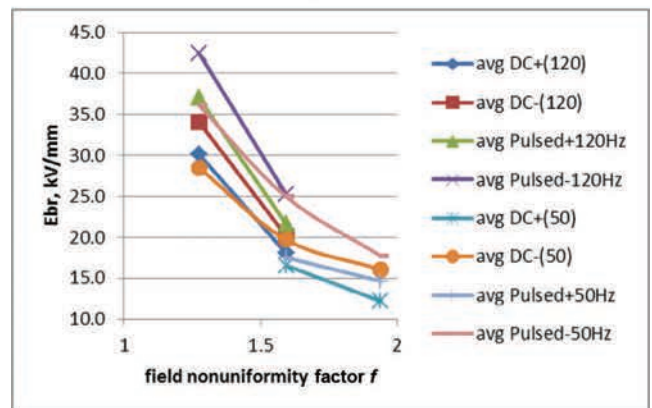
The results presented above suggest that, when designing oil insulation for pulsed conditions at frequencies up to at least 100 Hz, one can afford to decrease the insulation thickness by 10 to 20% relative to those required at DC. However, great care must be exercised because of the small number of tests carried



(a)



(b)



(c)

Figure 12. Test results (2011). (a) DC and pulsed test at PRR = 50 Hz, D = 20%. (b) DC and pulsed test at PRR = 120 Hz, D = 20%. (c) Dependence of the breakdown field  $E_{br}$  on field nonuniformity factor  $f$ . c is constructed using the data in a and b (note the uniformity of the data series legends in a, b, and c).

**Table 4. Percentage Increase in Breakdown Voltage (BV) for Pulsed Waveforms Relative to Their DC Counterpart [D = 50% at Pulse Repetition Rate (PRR) = 10 Hz, D = 20% for the Other PRRs].**

PRR, Hz	Polarity	
	Positive	Negative
10	15.6	10.4
30	14.9	10.3
50	12.0	16.6
120	19.3	22.2

out over a very limited parameter range. Only solid insoluble impurities were present in the oil under test, and the oil conditions were largely uncontrolled. It should also be recognized that much larger stressed oil volumes in real systems would result in lower breakdown voltages, compared with our test gap results (see Ch. 6 of [5]).

Since only solid impurities were present in the oil, one should consider the bridge mechanism of breakdown. For DC or pulses longer than, say, 50 ms, the particles can form a bridge that may initiate breakdown [1], [2], [4]–[7]. It can be argued that the findings of this work are consistent with this breakdown mechanism. At higher frequencies (30 to 120 Hz) breakdown occurred mainly on the leading edge of the pulse or immediately afterward, whereas at 10 Hz (and longer pulses) it occurred mainly on the flat top or the trailing edge of the pulse. Thus it took several tens of milliseconds to complete breakdown, which strongly suggests that slow processes were involved.

## Appendix

In this section, we quantify field nonuniformity in the test gap, and ground influence in the case of symmetrical connection. It is known that even distant ground may cause dramatic changes in the field distribution when least expected (see [17] for an example of a two-wire transmission line suspended high above ground, the distance between the wires being several orders of magnitude smaller than the distance to ground).

An analytical solution for the field on the axis of a sphere-to-sphere gap in symmetrical connection can be obtained in series

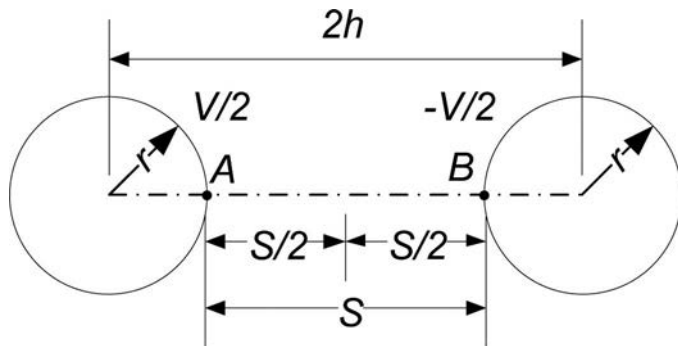


*Figure 13. Sphere-to-sphere gap geometry.*

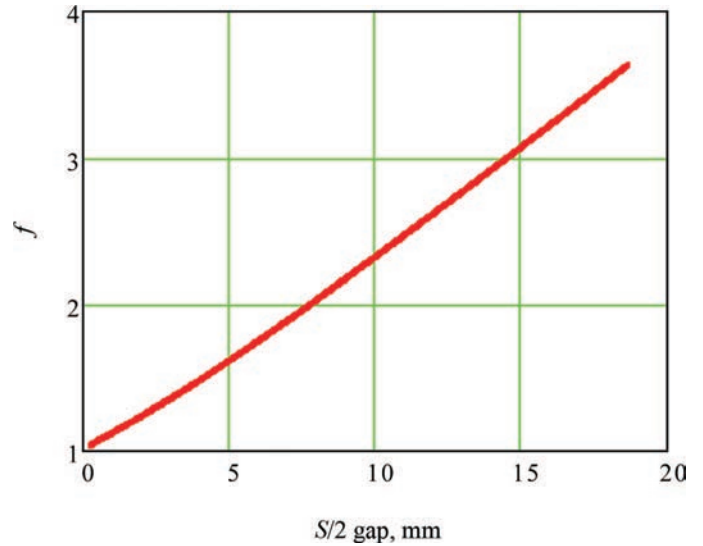


*Figure 14. Field nonuniformity factor  $f$  as a function of the sphere-to-plane gap  $S/2$ , with  $2r = 12.5$  mm (Figure 13).  $N =$  number of terms in series (2) = 1000.*

form, using the method of images [18]–[20]. The field maximum  $E_m$  is found at points A and B on the axis connecting the spheres (Figure 13). For symmetric connection

$$E_m = \frac{V}{2r} \frac{(1+x)^2}{1-x} \cdot \sum_{n=0}^N x^n \cdot \frac{1-x^{2n+1}}{(1+x^{2n+1})^2}, \quad (2)$$

where  $x = (h/r) - \sqrt{(h/r)^2 - 1}$  and  $V$  is the potential difference between the spheres (one at  $V/2$  and the other at  $-V/2$  relative to ground). The field nonuniformity factor  $f = E_m/E_{av}$ , where the average field in the gap  $E_{av} = V/S$ , and the gap is  $S = 2(h-r)$ .

Recognizing that the plane perpendicular to the axis and equidistant from the spheres is at zero potential, we can find the maximum field in the sphere-to-plane gap from (2) by halving the applied voltage and halving the gap width (see Figure 13). The field nonuniformity factor for a halved gap  $S/2$  is shown in Figure 14 for a range of gap widths.

Finite element analysis was used (Maxwell 2D Student Version [21]) to investigate the influence of the ground position on the field distribution. Using an axisymmetric approximation ( $R$ - $Z$  coordinates), we analyzed both symmetrical and asymmetrical connections. Some simulation examples are shown in Figures 15–18. Here,  $Z$  is the axis of rotation, and  $R$  is the radial coordinate. The positive electrode, a sphere mounted on a rod, is shown in red, and the negative electrode, a disc, is shown in blue (see Figure 3). Note that the case of symmetrical connection with an open boundary (Figure 18, zero voltage at infinity) is closest to the ideal case (Figure 13). It was found that the ground presence influences the field distribution only slightly, as do the HV leads, provided the gap is much smaller than the disk diameter. Thus,  $f$  in our tests can be reliably estimated from Figure 14. The discrepancy between analytical solutions obtained using

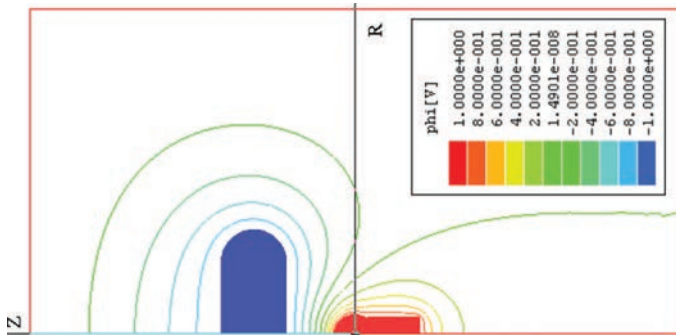


Figure 15. Field distribution with symmetrical connection, grounded boundary shown by red line. The positive electrode (a sphere mounted on a rod), shown in red, is held at potential  $\phi = 1$  V. The negative electrode (a disk), shown in blue, is held at  $\phi = -1$  V. Gap = 15 mm, field nonuniformity factor  $f = 2.8$ .

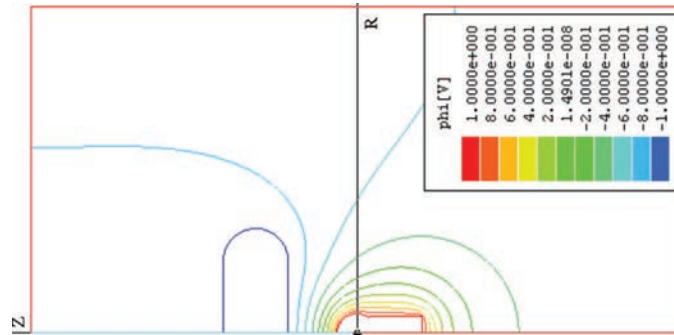


Figure 18. Field distribution with symmetrical connection, boundary open,  $f = 3.2$ , voltage  $\phi = 1$  V applied on the positive electrode (sphere mounted on a rod), voltage  $\phi = -1$  V applied on the negative electrode (a disk).

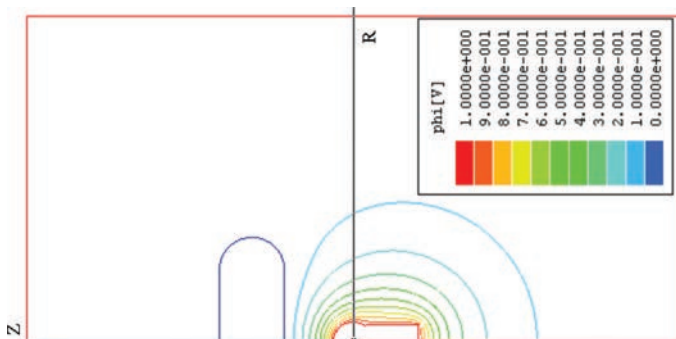


Figure 16. Field distribution with the negative electrode (a disk) and boundary grounded,  $f = 3.3$ , voltage  $\phi = 1$  V applied on the positive electrode (sphere mounted on a rod).

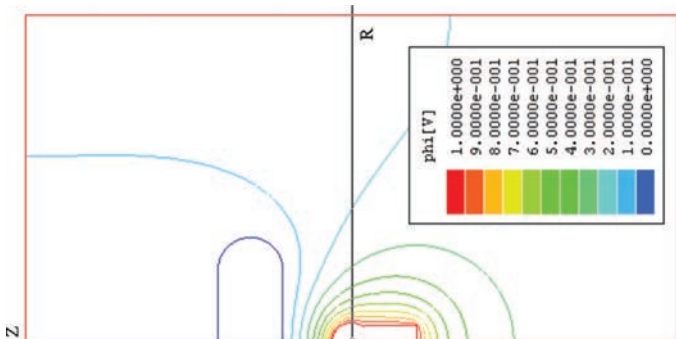


Figure 17. Field distribution with the negative electrode (a disk) grounded, boundary open,  $f = 3.15$ , voltage  $\phi = 1$  V applied on the positive electrode (sphere mounted on a rod).

(1) and (2), and those obtained using finite element analysis for a sphere-to-sphere gap, is typically less than 3% (field plot not shown).

## Acknowledgment

The authors thank Spellman High Voltage Electronics Corp. for support of this work.

## References

- [1] I. Adamczewski, *Ionization, Conductivity and Breakdown in Dielectric Liquids*, London, UK: Taylor & Francis, 1969.
- [2] T. J. Gallagher, *Simple Dielectric Liquids*, Oxford, UK: Clarendon Press, 1975.
- [3] T. J. Lewis, "Basic Electrical Processes in Dielectric Liquids," *IEEE Trans. Dielectr. Electr. Ins.*, vol. 1, no. 4, pp. 630–643, 1994.
- [4] G. I. Skanavi, *Physics of Dielectrics: Strong-Field Region*, Moscow, Russia: Fizmatlit, 1958.
- [5] V. Y. Ushakov, *Insulation of High-Voltage Equipment (Power Systems)*, Berlin, Germany: Springer, 2004. (Translation from Russian edition, 1994).
- [6] R. A. Lipshtein, and M. I. Shakhnovish, *Transformer Oil*, 3rd ed., Moscow, Russia: Energoatomizdat, 1983. (English translation of *Transformer Oil*, 2nd ed., Jerusalem, Israel: Israel Program for Scientific Translations, 1970).
- [7] V. Ya Ushakov, V. F. Klimkin, and S. M. Korobeynikov, *Impulse Breakdown of Liquids*, Berlin, Germany: Springer, 2007.
- [8] Power supply & x-ray tube in an integrated subsystem [Online]. Available: [http://www.spellmanhv.com/~media/Files/Downloads/Monoblock\\_catalog.ashx](http://www.spellmanhv.com/~media/Files/Downloads/Monoblock_catalog.ashx)
- [9] P. L. Bellaschi and W. L. Teague, "Dielectric Strength of Transformer Insulation," *Electr. Eng.*, vol. 56, no. 1, pp. 164–171, Jan. 1937.
- [10] SL Series of high voltage power supplies [Online]. Available: <http://www.spellmanhv.com/~media/Files/Products/SL.ashx>
- [11] *Test Method for Dielectric Breakdown Voltage of Insulating Oils of Petroleum Origin Using VDE Electrodes*, ASTM D 1816-84a, 1990.
- [12] <http://www.spellmanhv.com/~media/Files/Products/HVD.ashx>
- [13] *Insulating Liquids—Determination of the Breakdown Voltage at Power Frequency*, 2nd ed., IEC 156, 1995.
- [14] Insulation Liquid, by O. Hjortstam, T. Auletta, A. Jaksts, R. Liu, L. A. A. Pettersson, and L. Walfridsson (2008, Jun. 19), WIPO Patent Application WO/2008/071704.
- [15] J. G. Hwang, M. Zahn, F. M. O'Sullivan, L. A. A. Pettersson, O. Hjortstam, and R. Liu, "Electron scavenging by conductive nanoparticles in oil insulated power transformers," presented at 2009 Joint Electrostatics Conference, Boston, MA, Jun. 2009.

[16] J. G. Hwang, "Elucidating the Mechanisms Behind Pre-breakdown Phenomena in Transformer Oil Systems," PhD Thesis, MIT, Cambridge, MA, 2010.

[17] Pokryvailo, A., Yankelevich, Y., Nissim, N., Baksht, R., and Ashkenazy, J., "Development of Short Pulsed Corona on Two-Wire Transmission Line," *IEEE Trans. Plasma Sci.*, vol. 34, no. 1, pp. 104–114, Feb. 2006.

[18] G. I. Skanavi, *Physics of Dielectrics: Strong-Field Region*, Moscow, Russia: Fizmatlit, 1958.

[19] K. A. Rezvykh, "Calculation of electrostatic fields," *Energia*, vol. 34, no. 1, pp. 73–75, 1967.

[20] E. Kuffel and W. S. Zaengl, *High Voltage Engineering*, 2nd ed. Oxford, UK: Pergamon Press, 1984/2000.

[21] Maxwell 2D Student Version, Ansoft Corp., Pittsburgh, PA, 2002.

sis on high-current opening and closing switches and magnetic design, fast diagnostics, and corona discharges. Previously he studied switching arcs, designed SF<sub>6</sub>-insulated switchgear, and carried out research in the area of interaction of flames with electromagnetic fields. He has published more than 120 papers and two textbooks (in Hebrew), and holds more than 20 patents pertaining to HV technology.



**Alex Pokryvailo** was born in Vyborg, Russia. He received the M.Sc. and Ph.D. degrees in electrical engineering from the Leningrad Polytechnic Institute in 1975 and 1987, respectively. Formerly with Soreq Nuclear Research Center, Israel, he is now with Spellman High Voltage Electronics Corporation, serving as Director of

Research. His recent experience relates to design of HV high-power switch-mode power supplies, pulsed power with empha-



**Costel Carp** (IEEE Member since 2006) was born in Romania. He earned his B.Tek degree from Polytechnic Institute, Iasi, Romania, in 1986, and has been with Spellman High Voltage Electronics Corporation since 2002. His main field of expertise is power electronics, with emphasis on high-voltage, high-power supplies for industrial and medical applications.




---

## D E I S N E W S

---

The official DEIS website is <http://ewh.ieee.org/soc/deis/>. It contains comprehensive up-to-date information on the following:

- The DEIS—its structure, mission, and vision
- IEEE DEIS conferences—Directly sponsored IEEE DEIS conferences, to which a DEIS membership discount will apply, are marked with the DEIS logo.
- IEEE Electrical Insulation Magazine—Selected recent articles and editorials are briefly summarized, and links to the complete texts are provided. Guidelines on the preparation of articles for publication in the magazine and instructions for submitting an article can be downloaded.
- IEEE Transactions on Dielectrics and Electrical Insulation (TDEI)—The same materials are available as for the Electrical Insulation Magazine above.
- DEIS educational videos and DEIS chapter resources
- Career opportunities
- DEIS blogs, forums, and more!